

# Matching-Based Cercospora Leaf Spot Detection in Sugar Beet

Rong Zhou, Shun'ich Kaneko, Fumio Tanaka, Miyuki Kayamori, and Motoshige Shimizu

**Abstract**—In this paper, we propose a robust disease detection method, called adaptive orientation code matching (Adaptive OCM), which is developed from a robust image registration algorithm: orientation code matching (OCM), to achieve continuous and site-specific detection of changes in plant disease. We use two-stage framework for realizing our research purpose; in the first stage, adaptive OCM was employed which could not only realize the continuous and site-specific observation of disease development, but also shows its excellent robustness for non-rigid plant object searching in scene illumination, translation, small rotation and occlusion changes and then in the second stage, a machine learning method of support vector machine (SVM) based on a feature of two dimensional (2D) xy-color histogram is further utilized for pixel-wise disease classification and quantification. The indoor experiment results demonstrate the feasibility and potential of our proposed algorithm, which could be implemented in real field situation for better observation of plant disease development.

**Keywords**—Cercospora Leaf Spot (CLS), Disease detection, Image processing, Orientation Code Matching (OCM), Support Vector Machine (SVM).

## I. INTRODUCTION

SUGAR beet is a commercial plant which has been the second only to sugarcane as major source of global sugar production. However, foliar diseases in sugar beet often cause significant reduction in both quality and quantity and economic loss for sugar production. In particular, Cercospora leaf spot (CLS) is the most prevalent and destructive leaf in worldwide, and leads to major loss of gross sugar yield and less income for sugar factories and growers [1]. Therefore, this large economic demanding is the driving force for early detection and precise quantization of CLS in sugar beet, to timely and optimally determine the foliar fungicide application for reducing losses from CLS.

In general, the traditional way to decide the timing and quantity of CLS fungicide spraying is to monitor the field situation by aid of naked eye observation of disease specialists. And the objectives of the field monitoring are commonly divided into two phases: disease onset observation and spraying interval decision. The first fungicide application should occur at disease onset timing (the first spot is visible by human naked eye), which indicates the first phrase, and it plays vital role in

disease control management. This is because if the first application is late, control will be difficult all season, even if shorter than normal application intervals are used once applications start [2]. The other phase is to determine the subsequent fungicide spraying interval which mainly depends on the combination of disease severity evaluation and climate condition. Usually, the frequency and interval of the following fungicide applications are not constant, durable, profitable and eco-friendly control of CLS could be obtained if fungicides are adaptively applied according to some action thresholds, which mean to apply the fungicide at the timing of disease severity exceeding amount of threshold that can be tolerated in the field. Therefore, early detection and consecutive quantization of CLS in sugar beet are crucially demanded as the fundamental work for further sugar beet protection and environmental safety in both agriculture and horticulture field. However, these assignments require continuous monitoring and observation by disease specialists in the traditional way, which will be labor-intensive, prohibitively expensive, and subjective in large-scaled field. Furthermore, the farmers in some undeveloped agriculture counties may have to walk a long way to contract experts, which might be time consuming and costly.

To overcome this, automatic detection and quantization of plant disease is extremely required for precise plant protection under the large field scale. In recent years, image processing and machine vision techniques have been extensively explored for plant disease study for their merits of invasive, rapid, continuous and precise measurement capacities. Moreover, a number of inspiring algorithms have developed by image processing and computer vision techniques to detect, categorize, diagnose and quantize the plant disease in this multi-discipline field linking computer science with agriculture engineering.

A pixel-wise image registration was employed by using penalized likelihood warping and robust point matching methods with time sequence RGB and photosynthetic efficiency (PE) images of cabbage plant leaf in [3] for early predicting the outbreak of disease, which could deal with the leaf warping and slit overlapping problems during live leaf growing and moving processes. However, the method was only applied for a single leaf observation rather than a holistic plant which is more desirable to provide comprehensive information of plant in a field. Moreover, problems of leaf rotation and illumination changes during the realistic plant growth development were not taken into account. Camargo et al. [4] developed a disease segmentation algorithm by analyzing one dimensional (1D) distribution of intensity histogram to set a threshold by the position of a set of local maximums in the

Rong Zhou and Shun'ichi Kaneko are with the Division of Systems Science and Informatics, Hokkaido University, Sapporo, Japan. (phone: 011-706-6761; fax: 011-706-6761; e-mail: zhou@ssc.ssi.ist.hokudai.ac.jp).

Fumio Tanaka, Miyuki Kayamori, and Motoshige Shimizu are with the Central Agriculture Experiment Station, Hokkaido Research Organization, Naganuma, Japan.

histogram for diverse crop disease images identification. Furthermore, a continuous study was carried on and reported in [5] by using Support Vector Machine (SVM) to classify different disease causing agents of cotton crop based on RGB image. A set of feature such as shape, textures or fractal dimension were extract from different disease regions and best classification model with classification rate 93.1% was accessed via cross-validation. For improving the accuracy and stability of classifier model for disease classification by pattern recognition, Tian et al. [6] developed a SVM-based multiple classifier system (MCS) with color, texture and shape feature extracted from diverse disease regions to categorize different wheat leaf diseases. A better accuracy rate of 96.16% was demonstrated for the performance of the MCS with comparison of other pattern recognition methods. Hyperspectral imaging was used in [7] with eight vegetation indices related to physiological parameters based on image spectral reflection, as input of SVM classifier to detect disease at early stage and differentiate different pathogens caused sugar beet leaves. The potential of pre-symptomatic plant disease detection was demonstrated with the classification accuracy of 97% between healthy and disease leaves. Whereas the hyperspectral techniques are commonly costly and not portable to extend into the real field environment. Moreover, besides the disease detection and classification, few studies in the field of plant disease diagnosing could robustly, continuously and quantitatively provide the site-specific development of plant disease in a pixel-level, which is crucial and the challenge in precision agriculture for better disease observation and control.

To address these issues, in this paper, we propose a novel plant disease quantization algorithm based on a robust matching scheme called orientation code matching (OCM) [8] [9], which has shown its excellent performance in wide applications in areas like visual control [10], [11], medical imaging [12], surveillance [13], intelligent transport system [14] and other practical application. In order to continuously observe and study the site-specific disease development on leaves in a spatially coherent way, it is always difficult to handle the changes both in external environment (illumination variations, camera vibration) and internal plant circadian and growth (leave translation, small rotation, and occlusion). But the problems become simple by using the OCM method which could provide robust, continuous, and site-specific plant observation over time based on its template matching framework. In addition, by employing a pattern recognition approach of support vector machine (SVM) with our proposed two dimensional (2D) xy-color histogram feature, the pixel-wise quantization of plant disease development could also be assessed. In other words, this study shows its great potential to observe disease changes in plant health at anytime and anywhere.

## II. MATERIALS AND METHODS

### A. Experimental Treatment

#### 1. Plant Cultivation

The Sugar beet plants (cv. Amaibuki, 2004, Nippon beet

sugar manufacturing Co., Ltd., Japan) were cultivated in a ceramic pots (ø31cm) at 25/2°C (day/night), 15% relative humidity (RH) and with the help of daily spraying the water on the leaf surface for improving the RH. Plant were watered as necessary and fertilized every two weeks with 200ml of a 2% solution of fine powder HYPONeX (HYPONeX Co., Ltd., Japan).

Cercospora leaf spot (CLS) of sugar beet was chosen in this study as the specific disease detection due to its most economically important disease of sugar beets in worldwide. The disease is caused by the fungus *Cercospora beticola* which survives on infected crop residual as spores (conidiophores) and stromata. Under the favorable conditions, spores will germinate and penetrate the leaf surface to damage of the photosynthetic apparatus of leaf which will often begin from the symptom of an isolated leaf spot.

In this experiment, *Cercospora beticola* was infected by manually sprinkling the infected leaf residual on surface of the healthy plant leaves at the vegetative stage of sugar beet plant. Subsequently, the infected plants were put into plastic greenhouse to realize 90% RH at 25°C (day/night) for two weeks in order to produce conidiophores and experience through the incubation period.

#### 2. Experimental Configuration

An indoor experiment was conducted to assess health changes in sugar beet leaves under controlled conditions. The experiment system was settled next to the window of laboratory for utilizing the natural light to simulate the outdoor sunlight condition. The RGB plant images with 640×480 resolution were captured by a CMOS camera (CMOS130-USB2, Fortissimo Co., Japan) which was mounted on a horizontal beam supported by two vertical poles at a constant height of 1.9 m above the plant. The image captured from top view of plant canopy with the interval of each hour. An indoor fluorescent lamp was used for providing the light resource to capture the plant images during night period (17:00-6:00).

### B. Adaptive OCM for Continuous and Site-Specific Plant Observation

#### 1. Definition of OCM

OCM has been proposed as a robust image registration algorithm. It is defined as matching the orientation codes between two images which are to be compared for similarity evaluation.

For digital images, the orientation codes are obtained with quantized gradient angle of each pixel by applying some operator like for Sobel operator to compute the horizontal and vertical derivatives. If a discrete image is presented as  $I(x,y)$  then its gradient angle  $\theta_{x,y}$  could be obtained from:

$$\theta_{x,y} = \tan^{-1} \left( \frac{\nabla I_x}{\nabla I_y} \right) \quad (1)$$

where  $\nabla I_x = \frac{\partial I}{\partial x}$  and  $\nabla I_y = \frac{\partial I}{\partial y}$  are the horizontal and vertical gradient of pixel location  $(x,y)$ .

Then, orientation code (OC) is defined by quantizing  $\theta_{x,y}$  using a preset sector angle  $\Delta\theta$ :

$$c_{x,y} = \begin{cases} \left\lceil \frac{\theta_{x,y}}{\Delta\theta} \right\rceil: & |\nabla I_x| + |\nabla I_y| > \gamma \\ L: & |\nabla I_x| + |\nabla I_y| \leq \gamma \end{cases} \quad (2)$$

A separate code  $L (= \frac{2\pi}{\Delta\theta})$  is assigned for low contrast regions, for which it is not possible to compute the gradient angles. For all experiments, we used 16 ( $N = 16$ ) orientation codes ( $\Delta\theta = \frac{\pi}{8}$ ), which have been found to be the best through experiment evaluation. The threshold value  $\gamma$  plays an important role in suppressing the effect of noise and has to be selected according to the problem at hand. Small value of 10 was used for  $\gamma$  which was good for most of our experiment. A dissimilarity measurement is defined as the summation of the difference between the orientation codes of the corresponding pixels of the two regions being matched. The cyclic property of orientation codes is used for finding the difference. If  $O1(i,j)$  and  $O2(i,j)$  represent the orientation codes of the template image and any subimage from the scene, then the dissimilarity function between them is given by:

$$D = \frac{1}{M} \sum d(O1(i,j), O2(i,j)) \quad (3)$$

where  $M$  is the total number of pixels used in matching and  $d(\cdot)$  is the error function based on an absolute difference criterion:

$$d(m,n) = \begin{cases} \min(|m-n|, N-|m-n|): & m \neq N \cap n \neq N \\ 0: & m = n = N \\ \frac{N}{4}: & m \neq N \oplus n \neq N \end{cases} \quad (4)$$

In order to account for the differences in the quantization width, we normalize  $D$  by using maximum of error function  $\frac{N}{2}$  and refer to the result as dissimilarity  $D_{nor} = \frac{D}{\frac{N}{2}}$ .

Then the similarity is defined by using the dissimilarity  $D_{nor}$  as follows:

$$S = 1 - D_{nor} \quad (0 \leq S \leq 1) \quad (5)$$

## 2. Adaptive OCM for Continuous Plant Observation

Prior to disease detection and quantization, adaptive OCM was initially employed for the time sequence plant images for site-specific and continuous observation of disease development. An illustration of the above-mentioned procedure is given in Fig. 1.

Supposed  $T_{p,q}^{t-\Delta t}$  is the template at time  $t - \Delta t$  among the time sequence plant images, which  $(p,q)$  indicates the upper left position of the template and then searching its best match in the chronologically next plant image at  $t$  inside a window of pre-defined size within the neighbourhood around the center position of the  $T_{p,q}^{t-\Delta t}$ . The reason for setting a search window is that the motion and growth of plant between adjacent two

frames of plant images do not have severe variance. Consequently, the setting of the search window could not only improve the accuracy of matching result but also save the computation time. The size of the search window in this study is  $50 \times 50$  pixels.

Then the best match region  $T_{p+u,q+v}^t$  at time  $t$  is computed as following process and will be the adaptive template for searching object at time  $t + \Delta t$ : if  $O_{p,q}^{t-\Delta t}$  and  $O_{p+u,q+v}^t$  are the corresponding orientation code images for the images involved in the template matching, then the best matching position  $(p+u, q+v)$  at time  $t$  can be expressed as:

$$(u,v)_{p,q} = \arg \min_{x,y} D_{p,q}(x,y) \quad (6)$$

$$D_{p,q}(x,y) = \frac{1}{M} \sum_{i,j} d(O_{p,q}^{t-\Delta t}(i,j), O_{p+u,q+v}^t(i+x, j+y)) \quad \forall (p+x, q+y) \in W \quad (7)$$

where  $\Delta t$  is the image-capturing interval.  $W$ , centred at the former template position, whose size is pre-selected to accommodate the maximum expected displacement of template within plant image frames, is the search window for the adjacent template matching.

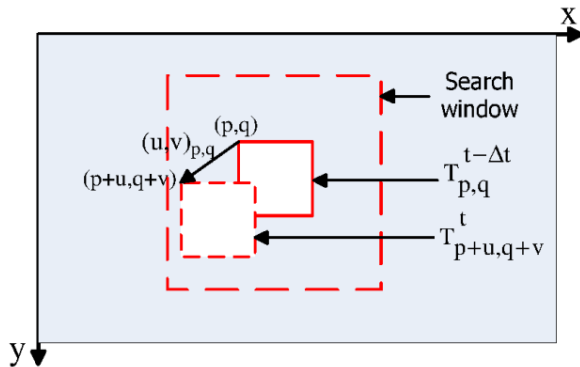


Fig. 1 An illustration of the adaptive OCM procedure

## C. Support Vector Machine (SVM) Classifier for Plant Disease Classification

By employing the template matching based on the adaptive OCM scheme, the site-specific information of plant leaves could be accessed for further plant health analysis. In this study, a machine learning method SVM was used to forward identify and quantify the disease development, by which could be involved in the application of decision-making of fungicide reduction.

### 1. Feature Definition and Extraction

A two dimensional (2D) xy-color histogram feature was introduced in this study for training SVM classification model to segment the disease pixels from healthy and their background pixels. We use a luminance-chromaticity CIE xyY color space rather than RGB color space because the former one could separately represent the luminance and chromaticity of the color. A CIE x-y chromaticity diagram could tell us the

chromaticity of a color in a “horseshoe” curve by eliminating the luminance component of the color, by which could provide more stable performance of object color information against illumination change. Figs. 2 (a) and (b) shows an intensity curve of a single pixel P (Fig. 2 (c)) in RGB and xyY color space individually from different plant images under various illumination changes. It can be seen that the R, G and B intensities of P are changing over large range due to light changes, whereas the x and y intensities are more stable due to eliminating the luminance information (intensity of Y) of object.

Based on the above color analysis, a 2D xy-color histogram is defined as the feature of SVM input for disease classification. For a template  $I_x(i, j)$  which is extracted from the plant image frame, its 2D xy-color histogram is given as:

$$H_{x,y} = P\{I_x(i, j) = x, I_y(i, j) = y\} \quad \forall (i, j) \in \text{template} \quad (8)$$

where  $(0 \leq I_x(i, j) \leq 1)$  and  $(0 \leq I_y(i, j) \leq 1)$  are the x and y color intensities in xyY color space. Fig. 3 demonstrates a comparable example of 2D xy-color histogram for templates belonging to disease, healthy and background (a white cardboard as background for eliminating the soil and pot resembles the color of CLS) respectively.

It can be seen that the 2D xy-color histogram shows a strong discriminative ability for segmenting the three different patterns. Therefore, the color intensity of x and y of image pixel was chosen and extracted as features for SVM classifier.

## 2. SVM Classifier

Support vector machine [15], [16] provides a solution for nonlinear two-class classification problems by mapping the training vectors into a higher dimensional space via a nonlinear mapping, and an optimal separate hyperplane can be constructed by the maximum margin between two sets of vectors. The Radial Basis Function (RBF) kernel was selected as kernel function for the nonlinear mapping in this study. When the classification problem involves more than two classes, several methods are available to extend dichotomous SVM classifier into multi-class classification. In this study, we use one-against-one [17] approach. The process of multi-classifier is to construct the classifiers for  $k(k-1)/2$  times, where  $k$  is the number of classes. Then each one is trained from data of two classes. Finally, the classification decision is made by a majority vote of the class assignments. If classes have identical votes, the one with the smallest index is selected.

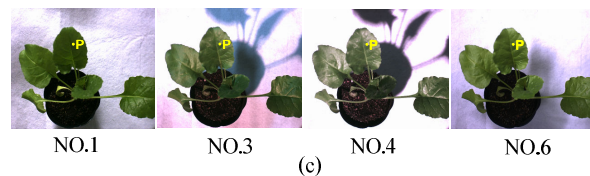
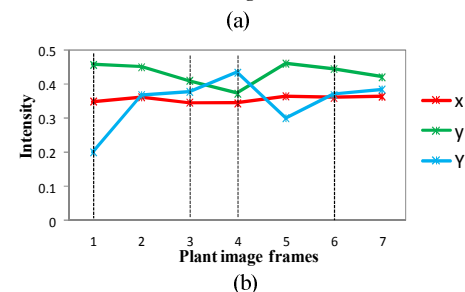
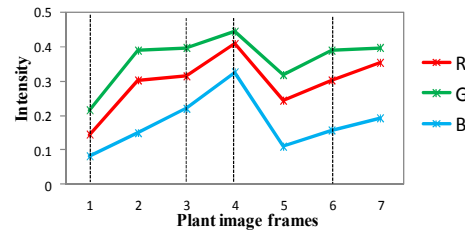


Fig. 2 Intensity curves of a single pixel  $P$  under various illumination conditions in RGB and xyY color space individually (a) RGB color space; (b) xyY color space; (c) illustration of the single pixel  $P$  in No.1, No.3, No.4 and No.6 plant image frames

## 3. Evaluation of the Classification Model

For optimizing and evaluating the SVM classifier, a training sample and testing sample were made as follow steps: firstly, one day captured plant images (00:00-23:00) were randomly chosen, of which 12 plant images from every two hour capturing interval were further as the image sets of training sample and testing sample; Then, 400 pixel-level x and y color intensities were extracted for each of three patterns (health, disease, white background) per image (that is  $400 \times 3$  pixels/image); Finally, all image data were divided into two sets: one is the training data at time of 2:00, 6:00, 10:00, 14:00, 18:00, 22:00, the other is test data at that of 0:00, 4:00, 8:00, 12:00, 16:00, 20:00. A desired classification accuracies (the proportion of correctly classified pixels in relation to all classified pixels) of 99.44% and 99.07% were obtained for training sample and testing sample respectively with the relative parameters setting are  $c = 4$ ,  $\sigma^2 = 2$ .

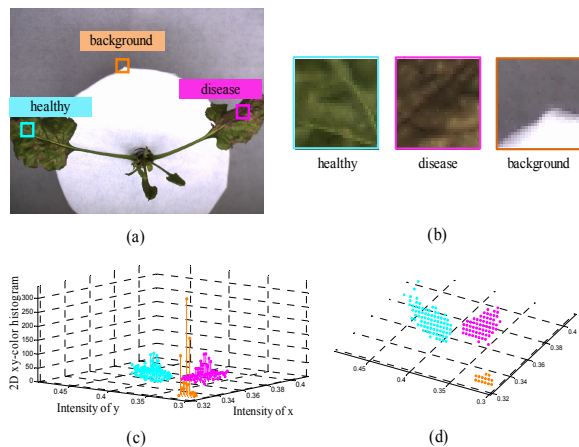


Fig. 3 A comparable examples of 2D xy-color histogram for templates belonging to disease, healthy and background respectively (a) three different templates extraction from plant image (b) the three templates of healthy, disease, and background (c) 2D xy-color histogram for the three patterns (d) the bird view of (c)

### III. EXPERIMENT RESULTS

In this section, experiment was implemented to evaluate the performance of our proposed method for continuous, site-specific and quantitative disease observation over time, compared with corresponding manually classification results.

#### A. Pixel-Wise Disease Segmentation and Quantization

For better observing the CLS disease changes in sugar beet, we chose one image per day as the observational interval during one-week period from 28th Dec, 2012 to 3rd Jan, 2013 (recorded as image frames: No.1-7) in this experiment. In addition, to observe the relationship between disease development process and its environmental RH, different amount of watering was sprayed on the plant leaves with a sprinkler at 1:00 am in each day. Five randomly chosen effective templates from the foremost plant frame on 28th Dec, 2012 in Fig. 4 (a) were implemented by our proposed algorithm for continuous and site-specific disease development observation over time. For demonstration the various illumination conditions of the seven plant frames, Fig. 4 (b) shows the average intensity of each frame. Clearly, illumination of each plant frame varies significantly and abruptly.

Fig. 5 (a) shows the disease classification and quantization results measured by proposed algorithm for the five effective templates over the week period. In addition, for evaluation and comparison the performance of the disease classification algorithm employed in this study, a similar result was assessed with manually classification (Fig. 5 (b)) under the guidance of the disease specialists. The similar growing trends of disease number for all five effective templates over time could be seen both in our proposed algorithm and manually classification results, which also corresponds to the mechanism of the CLS disease spreading. Moreover, the correlation between the extending speed of the CLS disease and its environmental

factor of RH could also be revealed: the CLS disease grows faster in higher RH condition than lower one. That is because spores of *Cercospora beticola* require moisture to germinate and infect leaves in much the same way that seeds require moisture to germinate and grow.

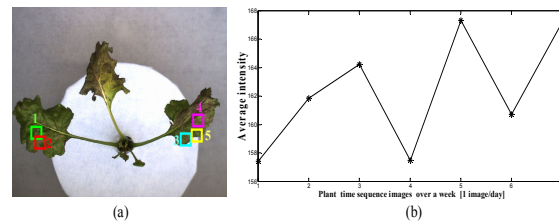


Fig. 4 Illustration of the five effective templates extraction and illumination conditions for plant frames over the experimental week period. (a) Extraction of five effective templates from plant image frame on Dec 28th, 2012 for disease development observation over time; (b) Average intensity for each plant frame among all plant time sequence images

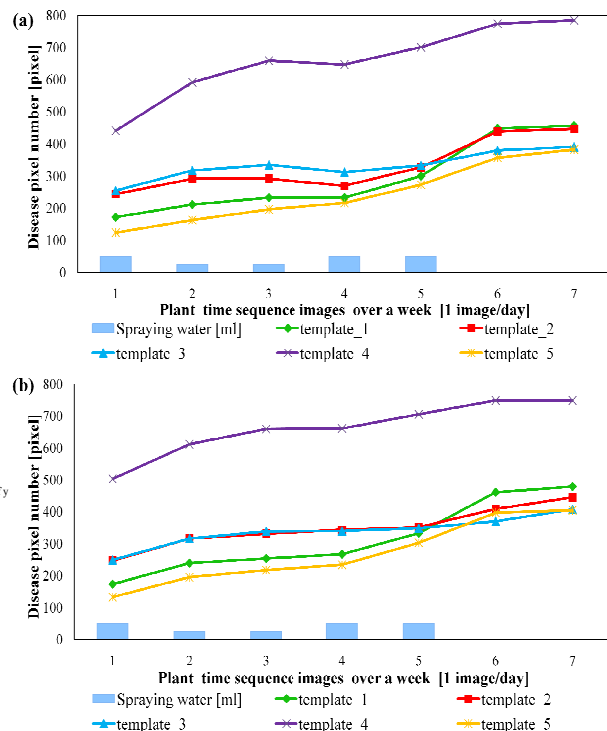


Fig. 5 Quantitative results for the disease development of the five effective templates, (a) by our proposed method, (b) by manually classification

Fig. 6 illustrates the visualization results of disease classification and its development process for two different effective templates (template\_1 and template\_3) of the five ones (template\_1-template\_5) in both image processing and manually segmentation approaches: 1) the disease in the first template (template\_1) is an isolated spot, it can be seen that the single spot was outward expanding both in size and shape over



time, and diffuses faster in the days with higher RH condition; 2) the disease in the third template (template\_3) initially started from one isolated and big spot, along with two isolated and small spots, as the disease processes, individual spots coalesce and heavily infected leaf tissue with size expanding. Therefore, it can be seen that the site-specific disease quantization and their expanding speed over time could be accessed by the proposed method, which will provide the information for

fungicide-spraying decision. Moreover, it could also help the disease specialists find out whether the applied fungicide is effective or not. However, from the contrastive visualization results compared with the manually classification, we could see that there is a distinct under-classification problem in the templates on Dec 31th, 2012. It might be attributed to the darker light condition in that day's plant image frame, which might lost its prior information in the training data.

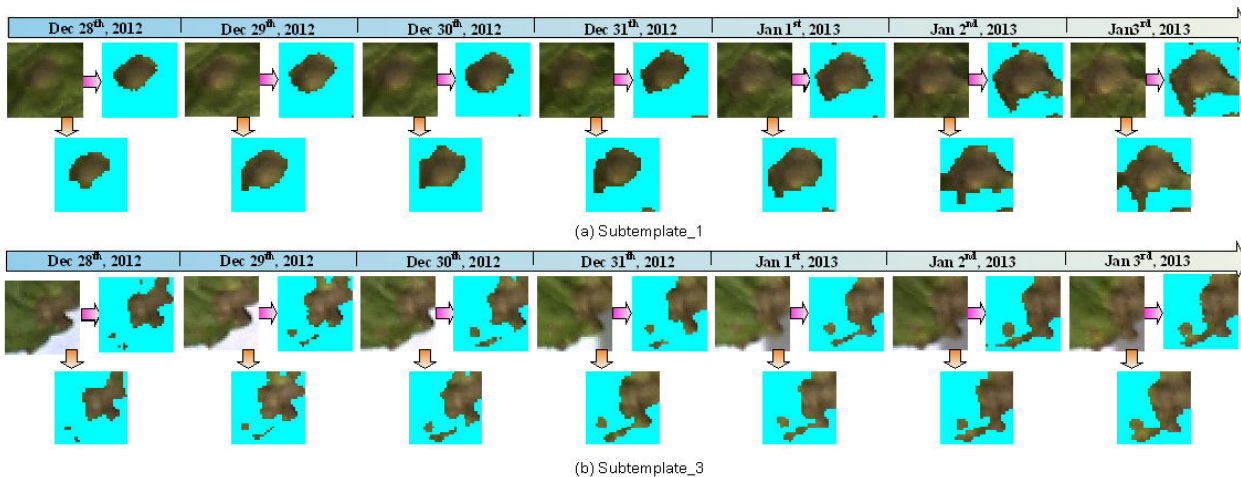


Fig. 6 Visualization result of disease classification and development process for two different effective templates of five. For the three images in each day, the upper left one indicates the RGB template image, upper right one is the corresponding disease classification result by our proposed method, and lower middle one is the result by manually classification. (a) shows the result of template\_1; (b) shows the result of template\_3. Blue areas correspond to disease region

### B. Algorithm Evaluation

Correlated to the manually disease classification results, three statistical measurements [18]: precision, recall and *F*-measure, are utilized in this study to analyze the temporal stability of the proposed method. In which precision can be seen as a measure of exactness of fidelity, while recall is a measure of completeness, and the *F*-measure considers both precision and the recall in computing the score, which could be interpreted and formulated as a weighted harmonic mean of precision and recall. The formulas for the three statistical measurements are:

$$\text{precision} = \frac{\text{TurePosition}}{\text{TurePosition} + \text{FalsePositive}} \quad (9)$$

$$\text{Recall} = \frac{\text{TurePosition}}{\text{TurePosition} + \text{FalseNegative}} \quad (10)$$

$$F = 2 \cdot \frac{\text{Precision} \cdot \text{Recall}}{\text{Precision} + \text{Recall}} \quad (11)$$

Comparative results of precision, recall and *F*-measure for the five templates are shown in Fig. 7. It can be seen that the classification accuracy for precision, recall and *F*-measure is consistent in a higher than the value of 0.74, which indicates the good performance and temporal stability of our proposed algorithm. But again, the lower value appears for all five templates on the fourth day (Dec 31th, 2012) over the one-week

period due to the darkest illumination condition.

In other words, by our proposed method, the site-specific, continuous and pixel-level quantifying of plant disease could be obtained for providing more precise information about the disease development, by which can lead us to optimally determine the timing and amount of fungicide spraying with climate condition. Moreover, our proposed method could also assist to judge the effect of the sprayed fungicide.

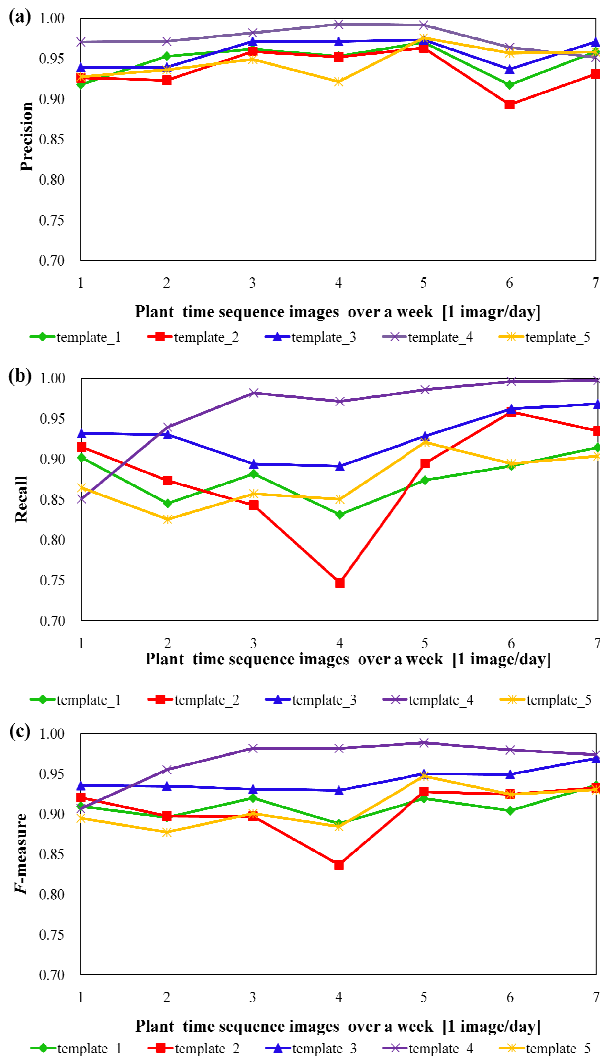


Fig. 7 Evaluation of the performance of our proposed method

#### IV. CONCLUSION

In this paper, we proposed a novel OCM-based algorithm for quantitatively deducing changes in plant health. Differing from the conventional plant disease analysis schemes, a robust matching scheme OCM was introduced in this study which could not only realize the continuous, site-specific observation of disease development, but also showed its excellent robustness for non-rigid plant object searching in scene illumination, live plant translation, small rotation and occlusion changes. The indoor experiment results, comparing the proposed method with manually classification, indicated the feasibility and potential of our proposed algorithm, which could be further implemented in real field situation for observing and quantifying the site-specific plant health development and fungicide spraying management. It should be also noted that this approach might be also generally applicable and suitable to other leafy plant varieties like cabbage and lettuce.

#### REFERENCES

- [1] W. W. Shane, P. S. Teng, "Impact of Cercospora leaf spot on root weight, sugar yield, and purity of Beta vulgaris", *Plant Dis.* Vol. 76, pp. 812-820, 1992.
- [2] J. Stachler, M. Khan, D. Franzen, M. Boetel, L. Smith, A. Sims, J. Lamb, A. Cattanaach, "Sugarbeet Production Guide", The Sugarbeet Research and Education Board of Minnesota and North Dakota, pp. 74-80, 2013.
- [3] G. Polder, G. W. A. M. van der Heijden, H. Jalink, J. F. H. Snel, "Correcting and matching time sequence images of plant leaves using Penalized Likelihood Warping and Robust Point Matching", *Computers and Electronics in Agriculture*, vol. 55, pp. 1-15, 2007.
- [4] A. Camargo, J. S. Smith, "An image-processing based algorithm to automatically identify plant disease visual symptoms", *Biosystems Engineering*, vol. 102, pp. 9-21, January, 2009.
- [5] A. Camargo, J. S. Smith, "Image pattern classification for the identification of disease causing agents in plants", *Computers and Electronics in Agriculture*, vol. 66, pp. 121-125, 2009.
- [6] Y. Tian, C. J. Zhao, S. L. lu, X. Y. Guo, "SVM-based Multiple Classifier System for recognition of wheat leaf diseases", *Intelligent Automation and Soft Computing*, vol. 15, No. X, pp. 1-10, 2009.
- [7] T. Rumpf, A. K. Mahlein, U. Steiner, E. C. Oerke, H. W. Dehne, L. Pumer, "Early detection and classification of plant disease with support vector machines based on hyperspectral reflectance", *Computers and Electronics in Agriculture*, vol. 74, pp. 91-99, 2010.
- [8] F. Ullah, S. Kaneko, S. Igarashi, "Orientation Code Matching for robust object search", *IEICE Trans. On Inf. & Sys*, E48-D, No. 8, pp. 999-1006, 2001.
- [9] F. Ullah, S. Kaneko, "Using orientation codes for rotation-invariant template matching", *Pattern Recognition*, vol. 37, pp. 201-209, 2004.
- [10] S. Hutchison, G. D. Hager, P. Coreke, "A tutorial introduction to visual servo control", *IEEE Trans. RA*, vol. 12, pp. 651-670, 1996.
- [11] N. Papanikolopoulos, P. Khosla, T. Kanade, "Visual tracking of a moving target by a camera mounted on a robot: A combination of control and vision", *IEEE Trans. RA*, vol. 9, pp. 317-328, 1993.
- [12] E. Bardinet, L. Cohen, N. Ayache, "Tracking medical 3D data with a deformable parametric model", *Proc. ECCV*, vol. 1, pp. 317-328, 1996.
- [13] R. Howarth, Buxton, "Visual surveillance monitoring and watching", *Proc. ECCV*, vol. 2, pp. 321-334, 1996.
- [14] T. Franc, M. Haag, H. Kollning, H. H. Nagel, "Traching of occluded vehicles in traffic scenes", *PROC. Eecv*, vol. 2, pp. 485-494, 1996.
- [15] N. V. Vapnik, *Statistical learning theory*, Wiley: New York, 1998.
- [16] N. V. Vapnik, *The nature of Statistical Learning Theory (Statistics for engineering and information science)*, 2nd ed., Springer-Verlag: New York, 2000.
- [17] S. Knerr, L. Personnaz, G. Dreyfus, "Single-layer learning revisited: a stepwise procedure for building and training a neural network". In *Neurocomputing*, Springer Berlin Heidelberg, pp. 41-50, 1990.
- [18] J. Makhoul, F. Kubala, R. Schwartz, R. Weischedel, "Performance measures for information extraction", In *Proceedings of DARPA Broadcast News Workshop*, pp. 249-252, 1999.